Supplementary Information for

Epigenetic editing by CRISPR/dCas9 in *Plasmodium falciparum*

Authors: Bo Xiao, Shigang Yin, Yang Hu, Maoxin Sun, Jieqiong Wei, Zhenghui Huang, Yuhao Wen, Xueyu Dai, Huiling Chen, Jianbing Mu, Liwang Cui, Lubin Jiang

Corresponding Authors: Lubin Jiang

Email: lbjiang@ips.ac.cn

This PDF file includes:

Supplementary Methods

Supplementary Figure S1 to S9

Supplementary Figure Legends S1 to S9

Tables S1

Supplementary Method References

www.pnas.org/cgi/doi/10.1073/pnas.1813542115

Supplementary Methods

5'-RACE.

The TSS of *eba-175* was mapped using the SMARTer® RACE 5'/3'Kit (Clontech) as described in the product user manual. Briefly, 1 µg of total RNA extracted from the 3D7 schizont was used to synthesize the first-strand cDNA in 20 µl of reaction with the First-Strand Buffer (50 mM DTT, 20 mM dNTP Mix, 0.5 µl RNase Inhibitor at 40 U/µl, and 100 U of SMARTScribe Reverse Transcriptase). 5'-cDNA end was amplified from 2.5 µl of 5'-RACE-Ready cDNA in 50 µl of 5'-RACE reaction with Universal Primer A Mix (0.2 µM gene specific primer, 25.0 µl of 2×SeqAmp Buffer, and 1.0 µl SeqAmp DNA Polymerase). The amplification was performed for 25 cycles of the conditions (94 °C for 30 s, 65 °C for 30 s, and 65 °C for 2 min). Three different gene specific primers (*SI Appendix*, Table S1) were successively used in a nest PCR program to verify the specific PCR products. The PCR products were cloned into the pRACE vector following the product user manual for sequencing.

RT-qPCR.

Total RNA of the schizonts (42-46 h) was extracted by using TRIzol (Life Technologies) for preparing the first strand cDNA with the FQ-RT primer Mix using a FastQuant RT Kit (TIANGEN) according to the product manual. qPCR was performed on a 384-wells Real-time PCR Detection System (ABI 7900HT) with a program of 1 cycle of 5 min at 95 °C; 40 cycles of 10 s at 95 °C, 20 s at 50 °C and 30 s at 60°C. The Relative RNA expression levels of each gene in the transfected parasites and the wild-type lines were normalized to the housekeeping gene seryl-tRNA synthetase (PF3D7_0717700) mRNA levels and calculated as $2^{\wedge} \triangle Ct$. All the qPCR primer sequences were listed in the *SI Appendix*, Table S1.

Indirect immunofluorescence assay (IFA).

The infected RBCs (iRBC) by *P. falciparum* at the trophozoite or schizont stage were first placed on coverslips pre-coated with poly-L-lysine for 30 min before fixation with 4% paraformaldehyde (ThermoFisher SCIENTIFIC) for 20 min at room temperature, and subsequently washed by 1×PBS for three times. The fixed cells were permeabilized by 0.25% Triton-100 (SIGMA) in 1×PBS for 15 min. After washing with 1×PBS, the

samples were blocked with the blocking solution of 5% BSA (Roche) in 1×PBS for 1 hour at room temperature and incubated with the blocking solution with 1:500 diluted mouse Monoclonal ANTI-FLAG® M2 antibody (SIGMA) at 4 °C overnight. After washing with 1×PBS for three times, the cells were further incubated with the blocking solution with 1:2,000 diluted Goat anti-Mouse IgG (H+L) Secondary Antibody (ThermoFisher SCIENTIFIC) at room temperature for another 1 hour followed by 1×PBS washing for three times. The labelled cells were mounted in the Fluoroshield Mounting Medium with DAPI (Abcam) and examined with an Olympus FV1200 Laser Scanning Microscope.

Western blotting.

Total proteins extracted from parasite pellets, which were pre-treated with 0.015% saponin for 10 min, were separated on 6-10% SDS-polyacrylamide gradient gels and blotted to a poly-vinylidene difluoride (PVDF) membrane (Millipore). The proteins was subsequently incubated with the blocking buffer (1×TBST with 5% nonfat milk) at room temperature for 1 h, the blocking buffer with 1:1000 diluted mouse anti-Cas9 (CST) at 4°C overnight, and the blocking buffer with 1:5,000 diluted Horseradish peroxidase-conjugated goat anti-mouse antibodies (The Jackson Laboratory), with three times washing by 1×TBST after each incubation. A mouse anti-Actin antibody (Abmart) was utilized to recognize the parasite actin, the sample loading control, at 1:1,000 dilution in the blocking buffer. The labelled proteins were visualized by using the Pierce™ ECL Western Blotting Substrate kit as described by the product manual (ThermoFisher SCIENTIFIC).

Cell invasion assay.

Parasite invasion assays were carried out in a 96-well plate cell culture system. Briefly, 4×10^5 schizont parasites were mixed with untreated, 1 mg/ml of chymotrypsin (Sigma) and 0.067 U/ml of neuraminidase (Millipore)-treated erythrocytes, respectively, at 2% hematocrit in 200 µl of Complete Medium under 5% O_2/5% CO_2/90% N_2 at 37 °C. Parasitemia of the ring stage parasites in the next asexual cycle was counted by a blood smearing and staining method.

Flow cytometry

Schizont parasites were isolated by a 70% Percoll/sorbitol (GE Healthcare) enrichment. At 4 h later, the 3D7 WT, 3D7-dCas9-GFP and 3D7-Sir2a-G1 parasites were synchronized with 5% sorbitol to obtain parasites with a 4 h IDC window. DNA content analysis was started in the early ring and carried out 6-10, 14-18, 22-26, 30-34, 38-42 hpi (hours post-invasion). Packed RBCs (40 µl) were fixed in 4% formaldehyde/0.015% glutaraldehyde for 30 min, washed three times in PBS and incubated for 20 min in 500 µl SYBR green staining solution diluted 1:5,000 in PBS (ThermoFisher SCIENTIFIC). Cells were washed three times in PBS prior to flow cytometry analysis using a MoFlo Astrios EQ instrument (BECKMAN COULTER). Ten thousand events (RBCs) were measured (excitation 488 nm; emission detection FL1 513 nm±26 nm), and a value of 5 on FL1 (SYBR green intensity) was applied as a threshold to identify (gate) iRBCs. Acquired data were processed using FlowJo software (v.10.0.5).

RNA-seq and data analysis.

Quantity and quality of the total RNAs (2-3 biological replicates) extracted from the schizont parasites were determined via a Bioanalyzer 2100 (Agilent) and a Qubit 2.0 Fluorometer (Life Technologies). Four µg of total RNA was used to prepare the cDNA library according to the KAPA Stranded mRNA-Seq Kit (Kapa Biosystems) production manual, with one adjustment of 62°C as the elongation temperature in PCR. The cDNA was proceeded for the paired-end (2×150 nt) genome-wide sequencing via an HiSeq X Ten sequencer (Illumina). All RNAseq raw data files were submitted to the Sequence Read Archive (SRA) database in NCBI (SRA Series accession number PRJNA493217). Paired-end 150-nt clean reads from each FASTQ file were mapped separately to *P. falciparum* reference genomes 3D7 or Dd2 by HISAT2 (version 2.0.5) using default parameters. In all samples, >95% of paired-end reads were specifically mapped to the genome. Differentially expressed transcript (DET) of each gene in Dd2-GCN5-R1, 3D7-Sir2a-E1 (3 biological repeats, in which the housekeeping ribosomal RNA genes were excluded) and 3D7-Sir2a-G1 (2 biological repeats) were identified against the transcriptomes of the wild-type parasites by using the R package DESeq2 with default parameters (1). Gene expression values were further normalized as the expression levels of genes based upon fragments per kilobase of exons per million fragments

mapped (FPKM) and evaluated for statistical significance by the Poisson distribution. Finally, each gene in Dd2-GCN5-R1 or 3D7-Sir2a-E1 against the wild-type parasite was presented as the scatter plot by the ggplot2 package (version 2.2.0) in R platform (version 3.2.4) using the logarithm FPKM values [log2(FPKM + 1)] as axes.

Downregulated genes resulted by repression of *PfSET1* were defined using the following criterion: $\log_2FC < -1$ and P value < 0.05, in which $\log_2FC$ represents the $\log_2$ fold change of 3D7-Sir2a-G1 strain comparing with the wild type strain calculated as $\log_2((FPKM^{3D7\text{-}Sir2a\text{-}G1} + 1) - \log_2(FPKM^{3D7\ WT} + 1))$. The P value is adjusted by the Benjamini method. The pie plot of the frequency distribution of phenotypes was drawn based on these downregulated genes. Phenotypes from their *P. berghei* orthologs were classified as Essential, Slow and Dispensable, respectively (2). In order to compare expression profiles of these *PfSET1*-regulated genes, gene expression values in FPKM at 8 time points post infection were analyzed using the public database (GEO accession number: GSE23787) (3). Scaled expression values were calculated as FPKM×scaling factors, which were adopted from the plasmoDB database (3). Briefly, the scaling factor are 0.0633, 0.05148, 0.06435, 0.18019, 0.64354, 0.89213, 1.0, 0.46349 corresponding to 5, 10, 15, 20, 25, 30, 35, 40 hpi (hours post infection). Heatmap of gene expression profiles was drawn according to the row-wise max values of each gene by using an in-house python script. All genes were sorted by the expression value (FPKM×scaling factor) of each row, which was normalized by z-score.

Genome-wide statistics of the dCas9 targets.

Genome-wide scanning of likely dCas9 targets (NGG/NGA) at the TSS regions (setting as 1500 bp upstream to 500 bp downstream of the mean sites of the TSS blocks) was executed using the customized scripts for Python language (version 2.7).

ChIP-seq data analysis.

Raw sequencing data analyzed in this study was downloaded from NCBI's Gene Expression Omnibus (GEO) at the GEO Series accession number GSE23787 (3). The H3K9 acetylation data in SRA format was converted by SRA Toolkit and trimmed for an average quality above 30. All reads in FASTQ format were mapped separately to the reference genome of *P. falciparum* 3D7 by using Bowtie2 (version 2.2.4) using the

default settings (4) with one adjustment at the command-line option allowing 1 mismatch (parameters "-p 8 -N 1"). More than 90% of the reads could be specifically mapped to the genome sequence, which was further filtered for duplicates using SAMtools (version 0.1.18). De-duplicated mapped reads were fed to MACS package (version 1.4) to find the enriched regions (peaks) over the genome using default parameters (5). H3K9ac ChIP peaks were annotated by Homer package (version 4.8) with our customized annotation GTF file and the genome data (6). Distribution profiles of histone acetylation in 500 genes with highest acetylation enrichment and another 500 genes with lowest acetylation enrichment at 4 different time points throughout the asexual stages of *P. falciparum* (10, 20, 30, 40 hpi) were plotted at the promoter regions (setting as 1,500 bp upstream to 500 bp downstream of the start codon of each gene) of the genes by compared to the TSS blocks (7).

153 # Supplementary Figures

154

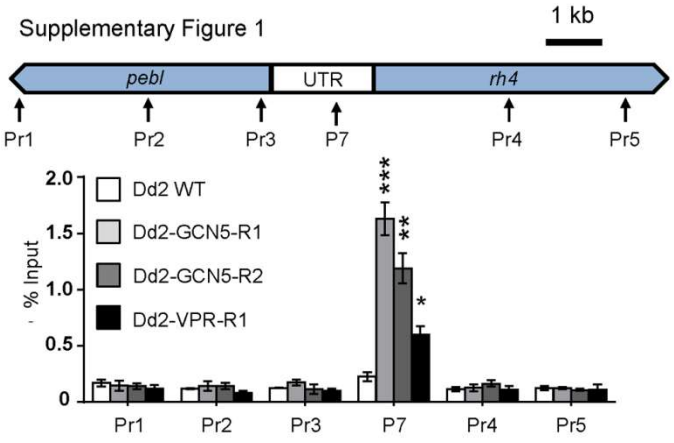

155

156

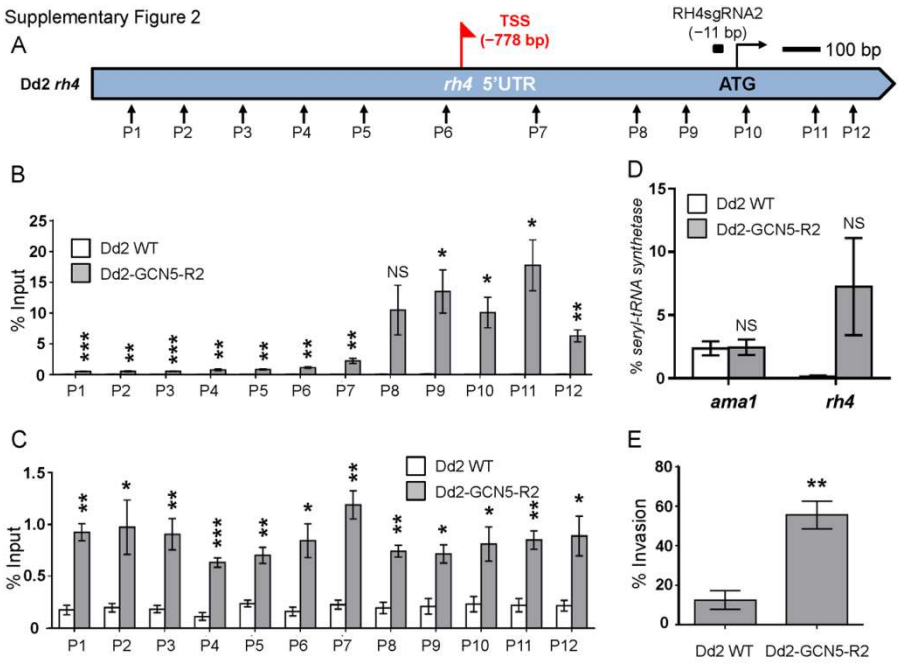
Supplementary Figure 2
A
TSS
(−778 bp)
RH4sgRNA2
(−11 bp)
100 bp
Dd2 rh4
rh4 5'UTR
ATG
P1 P2 P3 P4 P5 P6 P7 P8 P9 P10 P11 P12
B
% Input
Dd2 WT
Dd2-GCN5-R2
NS
C
% Input
Dd2 WT
Dd2-GCN5-R2
D
% seryl-tRNA synthetase
Dd2 WT
Dd2-GCN5-R2
NS
NS
ama1
rh4
E
% Invasion
Dd2 WT
Dd2-GCN5-R2
157

158

Supplementary Figure 3

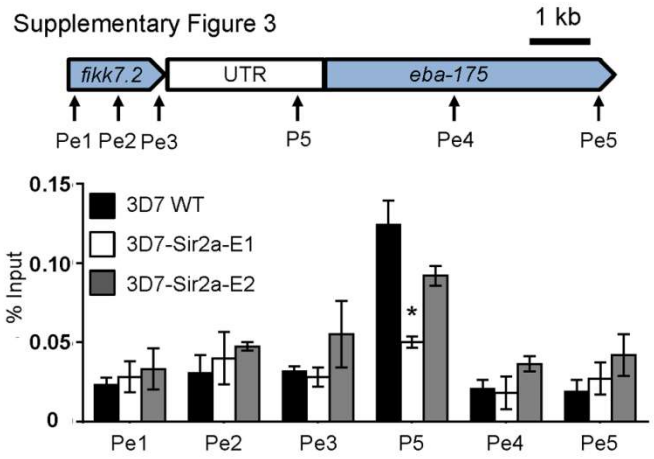

Supplementary Figure 4

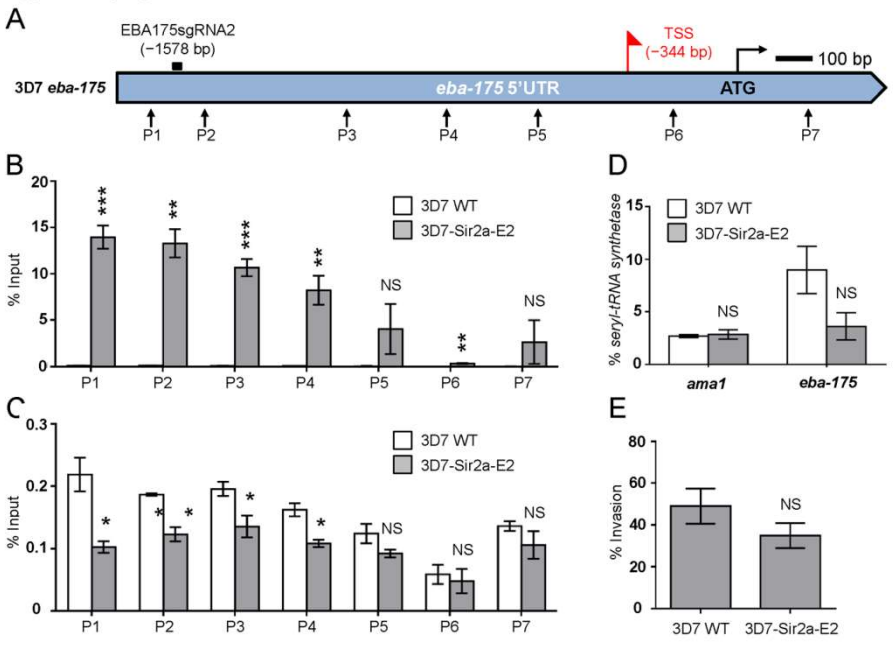

Supplementary Figure 5

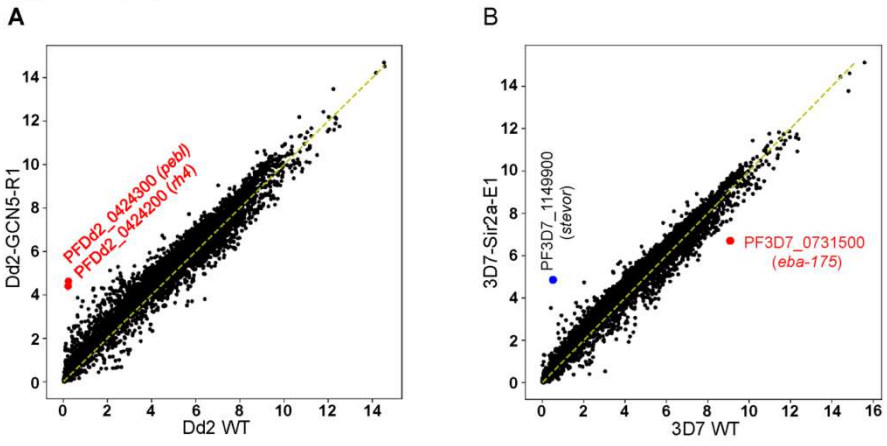

163

164

Supplementary Figure 6

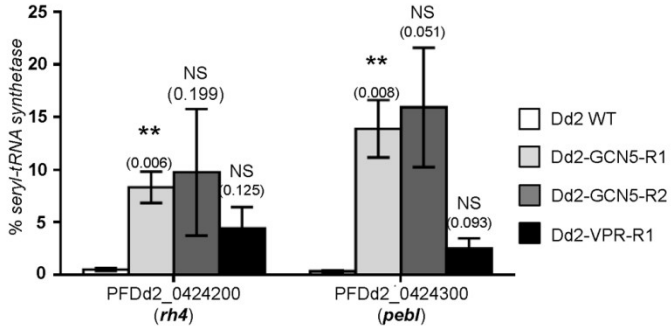

Supplementary Figure 7

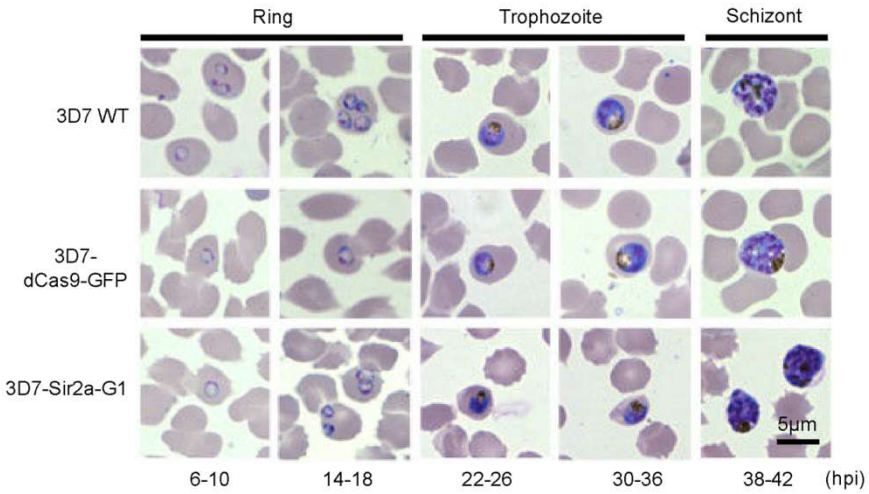

167

168

Supplementary Figure 8

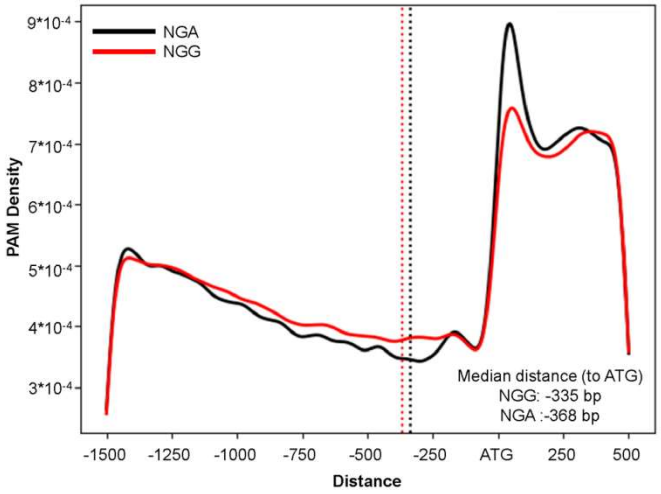

169

170

Supplementary Figure 9

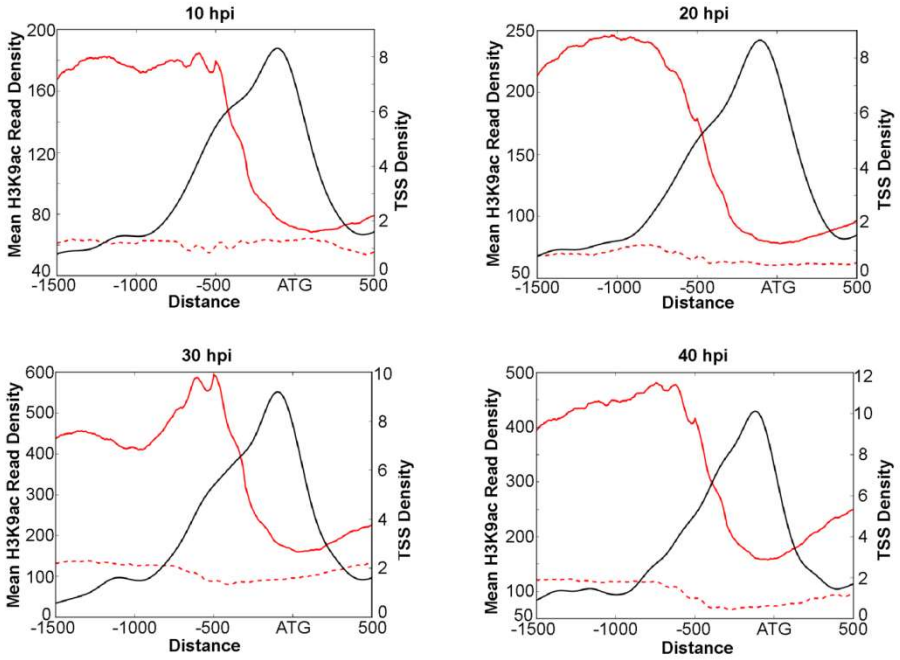

171

172

Supplementary Figure Legends

Figure S1. Authentication of histone 3 acetylation in Dd2-*rh4* by ChIP-qPCR. Schematic diagram of the six qPCR primer sets and the ChIP-qPCR analyses of schizont populations of cloned parasites derived from the Dd2 WT, Dd2-GCN5-R1, Dd2-GCN5-R2 and Dd2-VPR-R1 by using the anti-acetyl-histone H3 antibody. Experiments were biologically repeated three times. Error bars represent s.e.m. P values were obtained using an unpaired two-tailed Student's t-test. *P＜0.05, **P＜0.01, ***P＜0.001. Those without any annotation indicate no significant changes compared with the WT group.

Figure S2. Epigenetic regulation of the CRISPR/dCas9GCN5 guided by RH4 sgRNA2 on the *P. falciparum* gene *rh4*. (*A*) Schematic diagram of the gene activation strategy mediated by PfGCN5 in the CRISPR/dCas9 system. The position of the RH4sgRNA2 is shown as a black rectangle. The TSS site is shown as a red flag. (*B-C*) ChIP-qPCR analyses of schizont populations of cloned parasites derived from the Dd2-GCN5-R2 and the wild-type Dd2 (Dd2 WT) as a control, by using an anti-FLAG antibody (B) and an anti-acetyl-histone H3 antibody (*C*), respectively. (*D*) RT-qPCR analysis of the transcripts of *rh4* and *ama1* in Dd2-GCN5-R2 and the wild-type Dd2 at 44 hpi. Expression levels of *rh4* and *ama1* were normalized to expression of a housekeeping gene, *seryl-tRNA synthetase* (PF3D7_0717700). (*E*) Invasion efficiency of Dd2-GCN5-R2 and the wild-type Dd2 with different erythrocytes. The invasion rates of various parasite clones into the neuraminidase-treated erythrocytes were normalized to that of the same one into untreated erythrocytes set as 100%. Experiments were repeated three times. Error bars represent s.e.m. P values were obtained using unpaired two-tailed Student's t-test. ***P＜0.001, **P<0.01, *P<0.05. NS, not significant.

Figure S3. Authentication of histone 3 acetylation in 3D7-*eba175* by ChIP-qPCR. Schematic diagram of the six qPCR primer sets and the ChIP-qPCR analyses of schizont populations of cloned parasites derived from the 3D7 WT, 3D7-Sir2a-E1 and 3D7-Sir2a-E2 by using the anti-acetyl-histone H3 antibody. Experiments were biologically repeated three times. Error bars represent s.e.m. P values were obtained using an unpaired two-tailed Student's t-test, * P＜0.05, and those without any annotation means no significant changes compared with the WT group.

Figure S4. Epigenetic regulation of the CRISPR/dCas9Sir2a guided by EBA175 sgRNA2 on the *P. falciparum* gene *eba-175*. (*A*) Schematic diagram of the gene silencing strategy mediated by an epigenetic effector PfHDAC in the CRISPR/dCas9 system. P1-7, the seven primer sets for ChIP-qPCR. The position of the EBA175sgRNA2 is shown as a black rectangle. The TSS site is shown as a red flag. (*B-C*) ChIP-qPCR analyses of schizont populations of cloned parasites derived from the 3D7-Sir2a-E2 and the wild-type 3D7 (3D7 WT) as a control, by using an anti-FLAG antibody (B) and an anti-acetyl-Histone H3 antibody (*C*), respectively. (*D*) RT-qPCR analysis of the transcripts of *eba-175* and *ama1* in 3D7-Sir2a-E2 and the wild-type 3D7

at 44 hpi. Expression levels of *eba-175* and *ama1* were normalized to expression of a housekeeping gene, *seryl-tRNA synthetase* (PF3D7_0717700). (*E*) Invasion efficiency of 3D7-Sir2a-E2 and the wild-type 3D7 with the different erythrocytes. The invasion rates of various parasite clones into the chymotrypsin-treated erythrocytes were normalized to that of the same one into untreated erythrocytes set as 100%. Experiments were repeated three times. Error bars represent s.e.m. P values were obtained using unpaired two-tailed Student's t-test. ***P < 0.001, **P<0.01, *P<0.05. NS, not significant.

Figure S5. Global evaluation of off-target effects of the CRISPR/dCas9 systems in *P. falciparum*. (*A*) Comparative transcriptome analysis of wild-type Dd2 (Dd2 WT) and Dd2-GCN5-R1 at 44 h after invasion. X axis (wild-type Dd2) and y axis (Dd2-GCN5-R1) are logarithmic and correspond to differentially expressed transcript (DET) of each gene shown as a dot, which was normalized as the value of fragments per kilobase of exon per million fragments mapped (FPKM). *rh4* and its adjacent *pebl* are marked in red. (*B*) Comparative transcriptome analysis of wild-type 3D7 (3D7 WT) and 3D7-Sir2a-E1 at 44 hpi. X axis (wild-type 3D7) and y axis (3D7-Sir2a-E1) are logarithmic and correspond to DET of each gene shown as a dot, which was normalized as the value of FPKM. *eba-175* is marked in red. A potential off-target gene (PF3D7_1149900, *stevor*) is marked in blue.

Figure S6. Off-target effect authentication of *pebl* by RT-qPCR. The *rh4* and *pebl* genes in the wild-type Dd2 (WT), Dd2-GCN5-R1, Dd2-GCN5-R2 and Dd2-VPR-R1 at 44 hpi were analysis by RT-qPCR. Expression levels of the tested genes were normalized to expression of a housekeeping gene, *seryl-tRNA synthetase* (PFDd2_0717700). Experiments were biologically repeated three times. Error bars represent s.e.m. P values were obtained using unpaired two-tailed Student's t-test. **P＜0.01. NS, not significant.

Figure S7. Authentication of the phenotype change resulted by PfSET1 silencing. Microscopic morphology of the 3D7-Sir2a-G1, 3D7-dCas9-GFP and the wild-type 3D7 (3D7 WT) in Giemsa-stained thin blood smears at five consecutive time points from a single time course experiment. during the asexual stage. hpi, hours post infection. Scale bar, 5 μm.

Figure S8. Distribution of potential NGG and NGA PAM motifs among the 5'UTR of *P. falciparum* genes. A total of 261,196 NGG PAM motifs and 727,817 NGA PAM motifs within the potential promoter regions (setting as 1500 bp upstream to 500 bp downstream of the start codon) of *P. falciparum* genes were identified using the "NGG" and "NGA" seeds by a Python script customized in our lab. The density of PAM motifs (y axis) at a given distance (x axis) to the start codon "ATG" of each gene is plotted as red lines (NGA) and black lines (NGG). The red and black dashed lines indicate the median distance to the ATG for the NGA and NGG PAM motifs, respectively.

Figure S9. Average ChIP-seq signals over the promoter regions of *P. falciparum* genes

during the asexual stages. Distribution of histone H3K9 acetylation density (left *y* axis) from 500 genes with the highest H3 acetylation (red solid line) and 500 genes with lowest acetylation (red dashed line) is plotted at 10, 20, 30 and 40 hpi in *P. falciparum* (GSE: 23787) (3). Frequency of the TSS (right *y* axis) of each gene is plotted in a black solid line (7). X axis represents the distance to the ATG start codon of each gene.

Table S1: Primers used in this study

Primers Name	Sequences	Notes
D10A-F	AGAGTTGGTGCCGATAGCCAGGCCGATGCTGT	Point mutation
D10A-R	ACAGCATCGGCCTGGCTATCGGCACCAACTCT	
H840A-F	GCTCTGAGGCACGATTGCGTCCACATCGTAGTC	
H840A-R	ACTACGATGTGGACGCAATCGTGCCTCAGAGC	
bsd F	ATGCATGCCAAGCCTTTGTCTC	
bsd R	TTAGCCCTCCCACACATAACC	
GCN5 F	ATGCTGTTTATAAATGCCACG	Acetylation/deacetylation regulation domain
GCN5 R	TATAAAATGTATAGCTTTCTTTAC	
Sir2a F	ATGGGTAATTTAATGATTTCC	
Sir2a R	TTTCACTTGACCCTTTTAATATA	
GFP F	AGTAAAGGAGAAGAACTTTTC	GFP protein fusion
GFP R	TTATTTGTATAGTTCATCCATG	
EBA175 GSP 1	ATTACATATTGTTCTATAATCTGGCACCAGA	5’ RACE primer
EBA175 GSP 2	ACTTTAAACCTATAACATTTTCAATTCTAAACA	
EBA175 GSP 3	TGCAAAATATAACACAAAGAAGGAAGCA	
Universal Primer A Mix	CTAATACGACTCACTATAGGGCAAGCAGTGGTAT CAACGCAGAGT	
RH4 sgRNA1 F	AAATATAAACCTTACACAAG	sgRNA sequences
RH4 sgRNA1 R	CTTGTGTAAGGTTTATATTT	
RH4 sgRNA2 F	ATGGGTGTACTCATTCCTTA	
RH4 sgRNA2 R	TAAGGAATGAGTACACCCAT	
EBA175 sgRNA1 F	GATTATAGAACAATATGTAA	
EBA175 sgRNA1 R	TTACATATTGTTCTATAATC	
EBA175 sgRNA2 F	TTTTCAAGTTTACATAATTA	
EBA175 sgRNA2 R	TAATTATGTAAACTTGAAAA	
SET1sgRNA F	TTAAAAATTATAAACTGAGC	
SET1sgRNA R	GCTCAGTTTATAATTTTTAA	
Tel. sgRNA F	GGGTTTAGGGTTCAGGGTTT	
Tel. sgRNA R	AAACCCTGAACCCTAAACCC	
RH4 F	GTTCTTTTGTAGTTTCTAAC	mRNA expression qPCR primers
RH4 R	CGGAATCGAATCGTATTATG	
EBA175 F	GGAAGAGTTATGGAACTCCAG	
EBA175 R	GTAATAGTAACGATGCGATGTC	

AMA1 F	TAAGAACGCTAGTATGATCA	
AMA1 R	CCCTTACCATGACTTTTATA	
PF3D7_0629700 F	AAATCACAGTTGTGAGCCAA	
PF3D7_0629700 R	CTTCATGGGCTGCTATATCC	
PFDd2_0424300 F	GCAAATGGTAGAGAAGATCC	
PFDd2_0424300 R	GACATCTCTTCCAGAACTAC	
PF3D7_0717700 F	AAGTAGCAGGTCATCGTGGTT	
PF3D7_0717700 R	TTCGGCACATTCTTCCATAA	
Cas9 For	GATCATCGAGCAGATCAGCG	
Cas9 Rev	GTCAAAGTACTTGAAGGCGG	
EBA175 1F	ATGTATAATTTACTTGAAAAAGTTGC	3D7 *eba-175* ChIP-qPCR primer
EBA175 1R	AAAACCTAAATATAATAAGATCCTTG	
EBA175 2F	ATGACCTTCTAATTATTC	
EBA175 2R	CCTTGTTTTTATGGAATG	
EBA175 3F	TATATGGTTTTTCAAAAATAAACGTGC	
EBA175 3R	AAAAGCCTAAATATAATAAGATCCTTG	
EBA175 4F	AAGTGGTGTTCTAAAATATAATTAG	
EBA175 4R	TAAGAATTTTTTATAGAAAAGCACG	
EBA175 5F	AAAATAATTGTTTATTTTTATTAAGGAG	
EBA175 5R	TAAAAAATTCTAAAAAAATAACCATTAC	
EBA175 6F	GTGTAAATATTATAGTTG	
EBA175 6R	GTTAGTAAAAGAATATAAC	
EBA175 7F	ATGGAAATGTTCAAAAAACTGATAAG	
EBA175 7R	TTTTTATCTATATTATCTGGAGTTCC	
Pe1 F	AAAAATTGCTCAATACGTCG	
Pe1 R	ATTTAATCTTCCGAATAAGC	
Pe2 F	ATGCTGAAAATTATGTTATGG	
Pe2 R	AATCTTGGAAAATATTTTCTTG	
Pe3 F	TTAAAAAGACGAAAAGATGGC	
Pe3 R	ATTCTTCCTATAATCCATGTG	
Pe4 F	AAACAAGCATTGTCTACTTCAG	
Pe4 R	GAGATGTGATTGTAGATGATTC	
Pe5 F	ATACTTACAAAACTGCAAAAGTAAC	
Pe5 R	AATATAATAAATAACACACCTGCTC	
RH4 1F	TTTTTTTTATAGTTCTTATGTTATAGC	Dd2 *rh4* ChIP-qPCR primer
RH4 1R	TTATAGATGTGGTTTATGTACATAC	
RH4 2F	ATATTAGCCCTTTTTGTTTCTTC	
RH4 2R	ATATTTATGTGTGTGTATATTTTTG	
RH4 3F	TATTTATTTTACATGTAGAAACCTG	
RH4 3R	TTATTTATCGAAATAATATTGCACC	
RH4 4F	AATTCTAAGATCCTCCTTTCC	
RH4 4R	AATATTTTTAATATAAATAATTTTATTC	
RH4 5F	ATATTAAAAATATTATTAAGGTAAGTTC	

RH4 5R	CTTTTCTTTTCTTTTATTTCTCTATG	
RH4 6F	TTTTTTTTTTTATAATTATAGCATGTAC	
RH4 6R	TTTTATAAAAATAATATGTTCATTTTGTG	
RH4 7F	AATACATTTATATAATAAAAGAAGGAAG	
RH4 7R	AACTTTGTAATTCCATAAAGATGAG	
RH4 8F	TAAAAGATCTGGTTATATAAAAATC	
RH4 8R	ATTTTGTTTTTTCAAATGTTTGTTC	
RH4 9F	AATCGAATTTTTGTTAAGAACAAAC	
RH4 9R	ATGGAAGAAAAAAAAAATAAACAGAG	
RH4 10F	TTTTTTTTCTTCCATAAGGAATGAG	
RH4 10R	TTATATGTGTGTCGTTTTACTTATG	
RH4 11F	ACGACACACATATAATATAAACATG	
RH4 11R	TATATAAGTGTATGAAGGATATATG	
RH4 12F	GATATGTACCAAGGAAATGAC	
RH4 12R	GTGTGTTTTATTTATATCATGTTG	
Pr1 F	GCCTTTGAAGAAGCTAAT	
Pr1 R	CTTAATAATCCTATCCTATATGC	
Pr2 F	TATGTTTGATGGAAGACG	
Pr2 R	AATGATGTAATAAAGGAACCT	
Pr3 F	TGATAAGTTGGCAAATGG	
Pr3 R	TTCTCTGGAAGTTGTTCCT	
Pr4 F	ATATACAACAAACTACAAATCGG	
Pr4 R	GTAACCCAATTTTTTCATCATTC	
Pr5 F	CAAGAAGTTACAATATGAATGAGG	
Pr5 R	TTTTAAGACATTTGTCTTGTCTCC	

Supplementary Method References

1. Feng J*, et al.* (2012) GFOLD: a generalized fold change for ranking differentially expressed genes from RNA-seq data. *Bioinformatics* 28(21):2782-2788.
2. Bushell E*, et al.* (2017) Functional Profiling of a Plasmodium Genome Reveals an Abundance of Essential Genes. *Cell* 170(2):260-272 e268.
3. Bartfai R*, et al.* (2010) H2A.Z demarcates intergenic regions of the plasmodium falciparum epigenome that are dynamically marked by H3K9ac and H3K4me3. *PLoS pathogens* 6(12):e1001223.
4. Langmead B & Salzberg SL (2012) Fast gapped-read alignment with Bowtie 2. *Nature methods* 9(4):357-359.
5. Zhang Y*, et al.* (2008) Model-based analysis of ChIP-Seq (MACS). *Genome Biol* 9(9):R137.
6. Heinz S*, et al.* (2010) Simple combinations of lineage-determining transcription factors prime cis-regulatory elements required for macrophage and B cell identities. *Molecular cell* 38(4):576-589.
7. Adjalley SH, Chabbert CD, Klaus B, Pelechano V, & Steinmetz LM (2016) Landscape and Dynamics of Transcription Initiation in the Malaria Parasite Plasmodium falciparum. *Cell Rep* 14(10):2463-2475.